Inelastic Processes in Ne^+ and Ar^+ Collisions with Mg and Y Surfaces Leading to Scattered-Ion Fractions and Vacuum-Ultraviolet Photon Emission

J. Wayne Rabalais, Jie-Nan Chen, and Ranjit Kumar[a]
Department of Chemistry, University of Houston, Houston, Texas 77004
(Received 31 May 1985)

Collisions of kiloelectronvolt Ne^+ on Mg and Ar^+ on Y yield scattered-ion fractions as high as 70% and 38%, respectively, and $^{1,3}P \rightarrow {}^1S$ resonance radiation from the excited neutral projectile atoms in the vacuum-ultraviolet range 30–200 nm. These data, along with those from the oxidized and hydroxylated surfaces, show that electron promotions within the molecular orbitals of the quasidiatomic molecule formed during the close encounter are a significant, if not dominating, process in kiloelectronvolt ion-surface collisions.

PACS numbers: 79.20.Nc, 79.60.Cn

In ion-atom collisions in the kiloelectronvolt regime where electronic shells penetrate, purely elastic-scattering potentials cannot account for inelastic processes that result in electronic excitation and ionization. Such inelastic processes are typically observed as displacements in the scattering energy from the elastic position,[1-3] emission of electrons or photons,[4,5] and variations in the types and abundance of specific charge states of scattered species.[6,7] As part of our research efforts in understanding inelastic processes in ion-surface collisions, we have studied the vacuum-ultraviolet (VUV) photon emission and scattered-ion fractions f_i for 1–10-keV Ne^+ and Ar^+ bombardment of magnesium and yttrium surfaces. This work represents the first correlation of VUV photon emission and scattered-ion fractions during ion-surface collisions.

Most studies[8,9] of inelastic losses have been for gas-phase collisions and the Fano-Lichten (FL) mechanism[10] has been employed for interpretation. This mechanism is based on electron promotion[11] within molecular orbitals of a quasidiatomic molecule formed during collision. In more recent experiments[4] involving scattering from surfaces, the FL mechanism has been invoked to interpret observations of scattered-ion fractions and energy losses. As a result of the multitude of inelastic channels that exist on surfaces, the question of what inelastic channels are operative and dominant for ion-surface collisions remains unanswered. The data presented herein confirm the predictions of the FL mechanism for specific ion-surface atom combinations, hence strongly supporting the validity of the mechanism in kiloelectronvolt ion-surface inelastic processes.

There are few examples[12-15] of bombardment-induced photon-emission spectra in the VUV region. The spectra that do exist have been obtained with high-energy ions (50–600 keV), high ion fluxes (50–300 A/cm^2), and low-vacuum conditions (10^{-6}–10^{-7} Torr). These spectra reveal atomic line emission as well as continuous emission[12-14] from excited states of rare-gas dimers produced by interaction of implanted rare-gas atoms with the primary ion. The photon-emission spectra obtained here result from milder bombardment conditions (1–10 keV and 1–10 A/cm^2) and UHV (10^{-10} Torr).

The instrumental requirements for ion scattering with time-of-flight (TOF) analysis and the measurement of scattered-ion fractions have been described.[7] A Colutron ion source equipped with a Wien filter for mass selection, an off-axis aperature for elimination of neutrals, and an electronic chopper is used for primary ion-pulse formation. Scattering spectra are collected as a histogram of the distribution of particle flight times with use of a time-to-amplitude converter. Spectra of neutrals +ions and neutrals only (obtained by electrostatic deflection of the ions) were collected in alternating 20-sec intervals for periods of 10 min. The operating conditions are as follows: (1) primary beam 1–10 keV Ne^+ and Ar^+, 100-nsec pulse width, 0.5-nA/cm^2 ion current, and 50-kHz pulse rate; (2) 22° and 45° scattering angles and 6.5° incident angle from the surface; (3) ~3-kHz counting rate; (4) 2×10^{-10}-Torr base pressure. Photon emission as a result of the collisions was observed[4,16] in both the TOF scattering spectra and a 0.2-m UHV monochromator (situated at either 90° or 135° scattering angle) with a channel electron multiplier for detector in both cases. In the former case a single unmonochromatized photon peak is observed at zero flight time (on the microsecond scale) and in the latter case the range 30–200 nm was scanned (~200 nm is the upper wavelength limit of sensitivity for the multiplier).

The Mg sample was cut from 99.5%-purity rod and the Y sample was a thin foil of 99.9% purity. The samples were polished and cleaned by 3-keV Ar^+ bombardment with use of a separate sputter gun in the same chamber. Oxidized and hydroxylated surfaces were prepared by exposure to O_2 and H_2O as described previously.[16]

The spectral region 30–200 nm was scanned for 3-

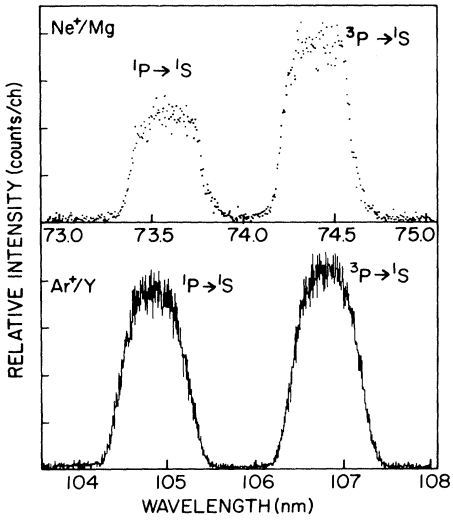

FIG. 1. Resonance radiation ($^{1,3}P \rightarrow {}^1S$) from excited Ne and Ar atoms resulting from 3-keV Ne^+ collisions with Mg and Ar^+ collisions with Y. The monochromator was set at 2 and 6 Å resolution for Ne and Ar, respectively. The spectrum resulting from Ne^+ collisions with Y is identical to the one shown here for Ne^+ on Mg.

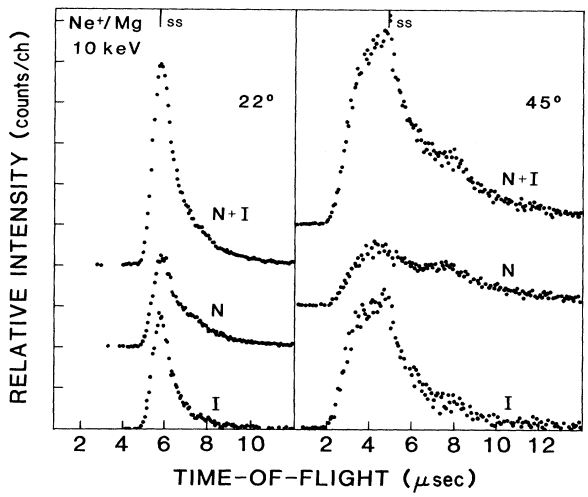

FIG. 2. TOF spectra for 10-keV Ne^+ scattering from Mg at 22° and 45° scattering angles. $(N+I)$, neutrals +ions; (N), neutrals; (I), $(N+I)-(N)$, ions. SS refers to the TOF corresponding to the calculated energy for single scattering from Mg atoms.

keV Ne^+ and Ar^+ bombardment of clean Mg and Y and for oxidized and hydroxylated Mg and Y. The results can be summarized as follows. (1) For clean Mg, no emission was observed with Ar^+ bombardment, while with Ne^+, intense $^{1,3}P \rightarrow {}^1S$ resonance radiation from neutral excited Ne at 73.6 and 74.4 nm was observed (Fig. 1). (2) For clean Y, the $^{1,3}P \rightarrow {}^1S$ resonance radiation from both excited neutral Ar and Ne were observed, Ar emission being at 104.8 and 106.7 nm (Fig. 1). (3) Emission from both singlet and triplet excited states (Fig. 1) exhibit comparable intensities. (4) For the oxidized and hydroxylated surfaces, the resonance radiation of (1) and (2) was reduced by about a factor of 2 and emission lines from excited O and H atoms were observed.

The photon spectra were measured under conditions of low primary flux and energy such that the concentration of implanted primaries and the flux of sputtered particles was minimized. The continua at 70–95 and 109.5–142.5 nm observed previously[12–14] for Ne^+ and Ar^+ bombardment, respectively, of metal surfaces is not observed as a result of the insufficient quantity of implanted rare gases. The comparable singlet-triplet emission intensities are unexpected on the basis of the lifetimes of the excited states for the gas-phase atoms. The abnormally high $^3P \rightarrow {}^1S$ transition intensity may be a result of selective population of the triplet relative to the singlet manifold and/or altered transition rates due to perturbations resulting from the close proximity of the surface. The latter point is expected to be significant in view of the large size of the Rydberg orbitals of these excited states.

The scattered-ion fractions f_i are strongly dependent on the distance of closest approach s_0, which is determined by the primary kinetic energy E_0 and the scattering angle θ. Typical TOF spectra for Ne^+ scattering from Mg at 22° and 45° are shown in Fig. 2 and f_i values at selected E_0 and θ are listed in Table I. The data can be summarized as follows: (1) For clean Mg, the f_i for Ne^+ are very high while those for Ar^+ are low. (2) For clean Y, the f_i for Ar^+ are moderately high while those for Ne^+ are low. (3) The high f_i values for Ne^+ on Mg and Ar^+ on Y are very sensitive to oxidation or hydroxylation, exhibiting a dramatic decrease (by $\sim$80%) upon chemisorption of O_2 and H_2O. The low f_i values of Ne^+ on Y and Ar^+ on

TABLE I. Scattered-ion fractions f_i and calculated distances of closest approach s_0.

Ion-target	θ	Ion Fraction (%)/s_0 (Å) 3 keV	5 keV	10 keV
Ne^+-Mg	22°	30.6/0.42	38.5/0.32	60.3/0.23
	45°	52.5/0.31	62.6/0.24	70.2/0.16
Ne^+-Y	22°	5.5/0.61	4.0/0.49	10.3/0.36
	45°	5.5/0.46	4.1/0.37	7.2/0.26
Ar^+-Mg[a]	22°	0.7/0.52	2.6/0.41	9.4/0.30
Ar^+-Y	22°	4.6/0.72	16.0/0.60	29.6/0.45
	45°	10.8/0.57	19.7/0.47	38.0/0.34

[a]Ion fractions were not measured for Ar^+-Mg at 45° because this is above the critical angle of 37° for single scattering of Ar from Mg.

Mg exhibit a minor increase ($\sim 10\%$) upon chemisorption.

Scattered-ion fractions and photons emitted as a result of ion-surface collisions can be treated[17] by division of the particle trajectory into three segments: (1) the incoming trajectory where resonant (RN) and Auger (AN) neutralization can occur, (2) the violent collision where the close encounter results in formation of a quasidiatomic molecule in which ionization, neutralization, and excitation of projectile and target atoms can occur, and (3) the outgoing trajectory where RN and AN are again possible. Neutralization into both ground and excited states of the ion occur by RN and AN processes along the incoming and outgoing trajectories as described by Hagstrum.[18] It has been shown that these neutralization probabilities are proportional to the amount of time that the ion spends near the surface (or inverse of the ion velocity component perpendicular to the surface). Such processes alone do not explain the results of our experiments.

Let us consider treatment in terms of electron promotion within the quasidiatomic molecule of the close encounter, as in application of the FL mechanism to gas-phase collisions. It has been shown[19] that inelastic energy losses are dependent on the distance of closest approach, $s_0(E_0, \theta)$. We have calculated s_0 by means of a scattering program[3] which uses the Molière approximation to the interaction potential. The calculated s_0 values are listed in Table I, along with the ion fractions. Lichten has shown[19] that for gas-phase Ne^+-Ne and Ar^+-Ar collisions, a sharp increase in the inelastic loss, number of ejected electrons, and excited atoms occurs at collision energies for which there is significant overlap of the L shells of the colliding pair. The sum of the radii of maximum radial charge density for the L shells is 0.59 Å for the Ne-Mg pair and 0.42 Å for the Ar-Mg pair. The s_0 values are within these critical internuclear distances for the Ne-Mg. For Ar-Mg the s_0 values are outside this critical range for 3-keV ions and barely within it for 5-keV ions.

The specific electron promotions in the close encounter can be predicted by construction of a separated-united atom diagram[11] and use of diabatic correlations[20] to determine electron configurations in the quasidiatomic molecule. Electrons promoted from filled shells into molecular orbitals (MO's) derived from atomic orbitals (AO's) of the separated atoms with higher principal quantum numbers can be trapped in these higher orbitals as the atoms separate, producing autoionizing and highly excited discrete states whose lifetimes (10^{-7}–10^{-8} sec) are longer than the collision times (10^{-13}–10^{-15} sec). The diagrams show that for such asymmetric atomic collisions, *the inner-shell excitation goes dominantly to the lighter, lower-atomic-number atom.*

For Ne-Mg collisions, Fig. 3, excitation energy can

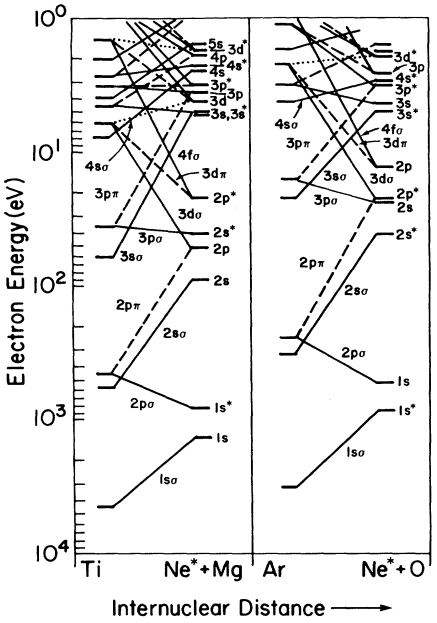

FIG. 3. United atom (UA)–separated atom (SA) correlation diagram for many electrons in the field of two differently charged nuclei. Diabatic MO's connect the levels of the infinitely separated atoms (right-hand side), maintaining the same value of the quantum number difference $(n-1)$. MO's with $M=0,1,2$ (σ, π, δ) are denoted by solid, dashed, and dotted lines, respectively.

be channeled into Ne through its $2p$ level which correlates with the highly promoted $4f\sigma$ MO. Electronic transitions from the $4f\sigma$ MO to other σ MO's can occur by radial coupling and transitions to π MO's can occur by rotational coupling. Autoionizing and excited states produced in this encounter are responsible for the large value of f_i and the large photon yield. Note that the $4f\sigma$-$3s\sigma$ crossing is the first and last orbital crossing to occur in the inward and outward trajectories, respectively. Promotion from the occupied $4f\sigma(2p$ AO) to the unoccupied $3s\sigma(3s$ AO) Rydberg orbital is a direct excitation path leading to the $(\ldots 2p^5 3s^1)^{1,3}P \rightarrow (\ldots 2p^6)^1S$ observed transitions.

For Ar-Mg collisions, excitation energy is channeled dominantly into Mg through its $2p$ level which correlates with the highly promoted $4f\sigma$ MO (diagram not shown); the resulting excited Mg atoms have a high probability of being quenched by their neighboring surface atoms. The low f_i values and lack of photon emission from excited Ar for Ar^+-Mg collisions is, hence, predicted by the model. An alternative explanation for the lack of Ar emission is the projectile-target mass ratio which allows no backscattering above the critical angle of 37°. Measurements (Table I) made at $\theta = 22°$ (well below the critical angle) exhibited a sharp single-scattering peak but no observable

photons, hence discounting the mass-ratio explanation.

For Ne and Ar collisions with Y, correlations similar to those of Fig. 3 show that excitation is channeled dominantly into the projectiles through promotion of the Ne $2p$ (correlating with the $5g\sigma$ MO) and Ar $3s$ and $3p$ (correlating with the $5d\sigma$ and $5f\sigma$ MO's). The lower f_i for Ne and higher f_i values for Ar scattering from Y (as compared to Mg) are in agreement with the predictions of Barat and Lichten[11]; that is, excitation cross sections should rise to a maximum for collision partners of similar atomic number Z and then decrease with increasing Z. The sensitivity of the high f_i values for Ne^+-Mg and Ar^+-Y to adsorbate coverage is due to the fact that collisions with the lighter adsorbate atoms on the surface result in channeling of excitation energy dominantly into the adsorbates rather than the heavier projectiles. For example, Fig. 3 shows that Ne^+-O collisions result in promotion of the O $2p$ AO which correlates with the $4f\sigma$ MO.

The molecular states and their related crossings must be considered in the analysis of the products of these collisions. As the atoms approach each other, molecular character evolves. Consider the specific case of Ne^+ on Mg; the Ne^+ ion approaches Mg along the $(NeMg)^+$ $[\ldots 2p^5\,{}^2P+\ldots 3s^2\,{}^1S]^2\Sigma, {}^2\Pi$ molecular ion potential surfaces corresponding to the MO configuration

$$1s\sigma^2 2p\sigma^2 2s\sigma^2 2p\pi^4 3p\sigma^2 3d\sigma^2 3d\pi^4 4f\sigma^2 3s\sigma^1.$$

If Ne^+ is neutralized into its ground or first excited state along the incoming trajectory, the approaches are along the (NeMg) $[\ldots 2p^6\,{}^1S+\ldots 3s^2\,{}^1S]^1\Sigma$ or $(NeMg)^*$ $[\ldots 2p^5 3s^1\,{}^3P+\ldots 3s^2\,{}^1S]^3\Pi$ molecular potential surfaces, respectively. These (NeMg) $^1\Sigma$, $(NeMg)^*\,{}^3\Pi$, and $(NeMg)^+\,{}^2\Sigma$, $^2\Pi$ molecular configurations correlate with excited states of Ti atoms that are several hundred electronvolts above the ground state of Ti. Similarly, if the Ti ground state $(\ldots 3d^2 4s^2\,{}^3F)$, first excited state $(3d^3 4s^1\,{}^5F)$, and ground ionic state $(3d^2 4s^1\,{}^4F)$ are correlated by means of diabatic MO's with AO's of separated atoms, highly excited autoionizing states of Ne and Mg result. Our conclusion is that there will be many crossings of NeMg, $(NeMg)^*$, and $(NeMg)^+$ states with excited molecular states that dissociate into excited and autoionizing atomic states with the result that electronic transitions in the close encounter will be the rule rather than the exception at close distances of approach.

Considerations of inelastic electronic processes occurring during the close atomic encounter are necessary for interpretation of our ion-fraction and photon-emission data resulting from kiloelectronvolt collisions. The dominant features of both the ion fractions and emitted photons can be traced to electron promotions in the quasimolecule of the close encounter. The Fano-Lichten mechanism[10,11] correctly predicts these features. It appears that the FL mechanism, modified to include charge-exchange transitions with the surface along the incoming and outgoing trajectories, is applicable to ion-surface collisions as well as gas-phase collisions (for which it was developed).

This material is based upon work supported by the National Science Foundation under Grant No. DMR-8304658.

---

[a]Present address: Analytical Research Division, W. R. Grace and Company, Columbia, Md.

[1]W. Eckstein, V. A. Molchanov, and H. Verbeek, Nucl. Instrum. Methods **149**, 599 (1978).

[2]S. B. Luitjens, A. J. Algra, E. P. Th. M. Suurmeijer, and A. L. Boers, Surf. Sci. **99**, 631 (1980).

[3]R. Kumar, M. H. Mintz, and J. W. Rabalais, Surf. Sci. **147**, 15 (1984).

[4]For recent reviews see E. W. Thomas, Vacuum **34**, 1031 (1984), and Prog. Surf. Sci. **10**, 383 (1980).

[5]R. A. Baragiola, Radiat. Eff. **61**, 47 (1982).

[6]T. M. Buck, G. H. Wheatley, and L. K. Verheij, Surf. Sci. **90**, 635 (1979).

[7]J. W. Rabalais, J. A. Schultz, R. Kumar, and P. T. Murray, J. Chem. Phys. **78**, 5250 (1983).

[8]J. C. Brenot, D. Dhuicq, J. P. Gauyacq, J. Pommier, V. Sidis, M. Barat, and E. Pollack, Phys. Rev. A **11**, 1245 (1975).

[9]B. Fastrup, G. Hermann, and K. J. Smith, Phys. Rev. A **3**, 1591 (1971).

[10]U. Fano and W. Lichten, Phys. Rev. Lett. **14**, 627 (1965).

[11]M. Barat and W. Lichten, Phys. Rev. A **6**, 211 (1972).

[12]M. Braun and B. Emmoth, Nucl. Instrum. Methods **170**, 585 (1980).

[13]K. W. Hill, J. Comas, D. J. Nagel, and A. R. Knudsen, Phys. Scr. **20**, 652 (1979); A. R. Knudson, D. J. Nagel, J. Comas, and K. W. Hill, Nucl. Instrum. Methods **149**, 507 (1978).

[14]R. S. Bhattacharya, K. G. Lang, A. Scharmann, and K. H. Schartner, J. Phys. D **11**, 1935 (1978); R. S. Bhattacharya, D. Hasselkamp, and K. H. Schartner, J. Phys. D **12**, L55 (1979).

[15]K. H. Schartner, H. J. Flaig, D. Hasselkamp, and A. Scharmann, Nucl. Instrum. Methods **168**, 419 (1980).

[16]J. A. Schultz, M. H. Mintz, T. R. Schuler, and J. W. Rabalais, Surf. Sci. **146**, 438 (1984).

[17]A. L. Boers, Nucl. Instrum. Methods **B4**, 98 (1984).

[18]H. D. Hagstrum, *Electron and Ion Spectroscopy of Solids,* edited by L. Fiermans, J. Vennik, and W. Dekeyser (Plenum, New York, 1978).

[19]W. Lichten, J. Phys. Chem. **84**, 2102 (1980).

[20]F. T. Smith, Phys. Rev. **179**, 111 (1969).